EUROPEAN ORGANIZATION FOR NUCLEAR RESEARCH

CERN-PPE/91-116
July 24, 1991

Decay Mode Independent Search for a Light Higgs Boson and New Scalars

The OPAL Collaboration

Abstract

Using data from e^+e^- collisions collected with the OPAL detector during the 1990 LEP run, a search was made for a low mass Higgs boson (H^0) with arbitrary decay mode. The existence of a Minimal Standard Model H^0 with mass in the range $0 \leq m_H \leq 11.3$ GeV/c^2 is excluded at the 95% confidence level for all possible decay modes of the H^0. Limits on the production of Higgs bosons predicted by the Minimal Supersymmetric Standard Model and new scalar particles that couple to the Z^0 are presented as a function of the scalar mass.

(Submitted to Physics Letters B)

The OPAL Collaboration

P.D. Acton[25], G. Alexander[23], J. Allison[16], P.P. Allport[5], K.J. Anderson[9], S. Arcelli[2], J.C. Armitage[6], P. Ashton[16], A. Astbury[a], D. Axen[b], G. Azuelos[18,c], G.A. Bahan[16], J.T.M. Baines[16], A.H. Ball[17], J. Banks[16], G.J. Barker[13], R.J. Barlow[16], J.R. Batley[5], G. Beaudoin[18], A. Beck[23], J. Becker[10], T. Behnke[8], K.W. Bell[20], G. Bella[23], S. Bethke[11], O. Biebel[3], U. Binder[10], I.J. Bloodworth[1], P. Bock[11], B. Boden[3], H.M. Bosch[11], S. Bougerolle[b], B.B. Brabson[12], H. Breuker[8], R.M. Brown[20], R. Brun[8], A. Buijs[8], H.J. Burckhart[8], P. Capiluppi[2], R.K. Carnegie[6], A.A. Carter[13], J.R. Carter[5], C.Y. Chang[17], D.G. Charlton[8], J.T.M. Chrin[16], P.E.L. Clarke[25], I. Cohen[23], W.J. Collins[5], J.E. Conboy[15], M. Cooper[22], M. Couch[1], M. Coupland[14], M. Cuffiani[2], S. Dado[22], G.M. Dallavalle[2], S. De Jong[8], P. Debu[21], L. Del Pozo[5], M.M. Deninno[2], A. Dieckmann[11], M. Dittmar[4], M.S. Dixit[7], E. Duchovni[26], G. Duckeck[11], I.P. Duerdoth[16], D.J.P. Dumas[6], G. Eckerlin[11], P.A. Elcombe[5], P.G. Estabrooks[6], E. Etzion[23], F. Fabbri[2], M. Fincke-Keeler[a], H.M. Fischer[3], D.G. Fong[17], C. Fukunaga[24], A. Gaidot[21], O. Ganel[26], J.W. Gary[11], J. Gascon[18], R.F. McGowan[16], N.I. Geddes[20], C. Geich-Gimbel[3], S.W. Gensler[9], F.X. Gentit[21], G. Giacomelli[2], V. Gibson[5], W.R. Gibson[13], J.D. Gillies[20], J. Goldberg[22], M.J. Goodrick[5], W. Gorn[4], C. Grandi[2], F.C. Grant[5], E. Gross[26], J. Hagemann[8], G.G. Hanson[12], M. Hansroul[8], C.K. Hargrove[7], P.F. Harrison[13], J. Hart[5], P.M. Hattersley[1], M. Hauschild[8], C.M. Hawkes[8], E. Heflin[4], R.J. Hemingway[6], R.D. Heuer[8], J.C. Hill[5], S.J. Hillier[1], D.A. Hinshaw[18], C. Ho[4], J.D. Hobbs[9], P.R. Hobson[25], D. Hochman[26], B. Holl[8], R.J. Homer[1], S.R. Hou[17], C.P. Howarth[15], R.E. Hughes-Jones[16], R. Humbert[10], P. Igo-Kemenes[11], H. Ihssen[11], D.C. Imrie[25], L. Janissen[6], A. Jawahery[17], P.W. Jeffreys[20], H. Jeremie[18], M. Jimack[2], M. Jobes[1], R.W.L. Jones[13], P. Jovanovic[1], D. Karlen[6], K. Kawagoe[24], T. Kawamoto[24], R.K. Keeler[a], R.G. Kellogg[17], B.W. Kennedy[15], C. Kleinwort[8], D.E. Klem[19], T. Kobayashi[24], T.P. Kokott[3], S. Komamiya[24], L. Köpke[8], R. Kowalewski[6], H. Kreutzmann[3], J. von Krogh[11], J. Kroll[9], M. Kuwano[24], P. Kyberd[13], G.D. Lafferty[16], F. Lamarche[18], W.J. Larson[4], J.G. Layter[4], P. Le Du[21], P. Leblanc[18], A.M. Lee[17], M.H. Lehto[15], D. Lellouch[8], P. Lennert[11], C. Leroy[18], L. Lessard[18], J. Letts[4], S. Levegrün[3], L. Levinson[26], S.L. Lloyd[13], F.K. Loebinger[16], J.M. Lorah[17], B. Lorazo[18], M.J. Losty[7], X.C. Lou[12], J. Ludwig[10], M. Mannelli[8], S. Marcellini[2], G. Maringer[3], A.J. Martin[13], J.P. Martin[18], T. Mashimo[24], P. Mättig[3], U. Maur[3], J. McKenna[a], T.J. McMahon[1], J.R. McNutt[25], F. Meijers[8], D. Menszner[11], F.S. Merritt[9], H. Mes[7], A. Michelini[8], R.P. Middleton[20], G. Mikenberg[26], J. Mildenberger[6], D.J. Miller[15], R. Mir[12], W. Mohr[10], C. Moisan[18], A. Montanari[2], T. Mori[24], M.W. Moss[16], T. Mouthuy[12], B. Nellen[3], H.H. Nguyen[9], M. Nozaki[24], S.W. O'Neale[8,d], B.P. O'Neill[4], F.G. Oakham[7], F. Odorici[2], M. Ogg[6], H.O. Ogren[12], H. Oh[4], C.J. Oram[e], M.J. Oreglia[9], S. Orito[24], J.P. Pansart[21], B. Panzer-Steindel[8], P. Paschievici[26], G.N. Patrick[20], S.J. Pawley[16], P. Pfister[10], J.E. Pilcher[9], J.L. Pinfold[26], D.E. Plane[8], P. Poffenberger[a], B. Poli[2], A. Pouladdej[6], E. Prebys[8], T.W. Pritchard[13], H. Przysiezniak[18], G. Quast[8], M.W. Redmond[9], D.L. Rees[1], K. Riles[4], S.A. Robins[13], D. Robinson[8], A. Rollnik[3], J.M. Roney[9], E. Ros[8], S. Rossberg[10], A.M. Rossi[2,f], P. Routenburg[6], K. Runge[10], O. Runolfsson[8], D.R. Rust[12], S. Sanghera[6], M. Sasaki[24], A.D. Schaile[10], O. Schaile[10], W. Schappert[6], P. Scharff-Hansen[8], P. Schenk[a], H. von der Schmitt[11], S. Schreiber[3], J. Schwarz[10], W.G. Scott[20], M. Settles[12], B.C. Shen[4], P. Sherwood[15], R. Shypit[b], A. Simon[3], P. Singh[13], G.P. Siroli[2], A. Skuja[17],

A.M. Smith[8], T.J. Smith[8], G.A. Snow[17], R. Sobie[g], R.W. Springer[17], M. Sproston[20], K. Stephens[16], H.E. Stier[10], R. Ströhmer[11], D. Strom[9], H. Takeda[24], T. Takeshita[24], P. Taras[18], S. Tarem[26], P. Teixeira-Dias[11], N.J. Thackray[1], G. Transtromer[25], T. Tsukamoto[24], M.F. Turner[5], G. Tysarczyk-Niemeyer[11], D. Van den plas[18], R. Van Kooten[8], G.J. VanDalen[4], G. Vasseur[21], C.J. Virtue[19], A. Wagner[11], C. Wahl[10], J.P. Walker[1], C.P. Ward[5], D.R. Ward[5], P.M. Watkins[1], A.T. Watson[1], N.K. Watson[8], M. Weber[11], P. Weber[6], S. Weisz[8], P.S. Wells[8], N. Wermes[11], M. Weymann[8], M.A. Whalley[1], G.W. Wilson[21], J.A. Wilson[1], I. Wingerter[8], V-H. Winterer[10], N.C. Wood[16], S. Wotton[8], T.R. Wyatt[16], R. Yaari[26], Y. Yang[4,h], G. Yekutieli[26], I. Zacharov[8], W. Zeuner[8], G.T. Zorn[17].

[1]School of Physics and Space Research, University of Birmingham, Birmingham, B15 2TT, UK
[2]Dipartimento di Fisica dell' Università di Bologna and INFN, Bologna, 40126, Italy
[3]Physikalisches Institut, Universität Bonn, D-5300 Bonn 1, FRG
[4]Department of Physics, University of California, Riverside, CA 92521 USA
[5]Cavendish Laboratory, Cambridge, CB3 0HE, UK
[6]Carleton University, Dept of Physics, Colonel By Drive, Ottawa, Ontario K1S 5B6, Canada
[7]Centre for Research in Particle Physics, Carleton University, Ottawa, Ontario K1S 5B6, Canada
[8]CERN, European Organisation for Particle Physics, 1211 Geneva 23, Switzerland
[9]Enrico Fermi Institute and Department of Physics, University of Chicago, Chicago Illinois 60637, USA
[10]Fakultät für Physik, Albert Ludwigs Universität, D-7800 Freiburg, FRG
[11]Physikalisches Institut, Universität Heidelberg, Heidelberg, FRG
[12]Indiana University, Dept of Physics, Swain Hall West 117, Bloomington, Indiana 47405, USA
[13]Queen Mary and Westfield College, University of London, London, E1 4NS, UK
[14]Birkbeck College, London, WC1E 7HV, UK
[15]University College London, London, WC1E 6BT, UK
[16]Department of Physics, Schuster Laboratory, The University, Manchester, M13 9PL, UK
[17]Department of Physics and Astronomy, University of Maryland, College Park, Maryland 20742, USA
[18]Laboratoire de Physique Nucléaire, Université de Montréal, Montréal, Quebec, H3C 3J7, Canada
[19]National Research Council of Canada, Herzberg Institute of Astrophysics, Ottawa, Ontario K1A 0R6, Canada
[20]Rutherford Appleton Laboratory, Chilton, Didcot, Oxfordshire, OX11 0QX, UK
[21]DPhPE, CEN Saclay, F-91191 Gif-sur-Yvette, France
[22]Department of Physics, Technion-Israel Institute of Technology, Haifa 32000, Israel
[23]Department of Physics and Astronomy, Tel Aviv University, Tel Aviv 69978, Israel
[24]International Centre for Elementary Particle Physics and Dept of Physics, University of Tokyo, Tokyo 113, and Kobe University, Kobe 657, Japan
[25]Brunel University, Uxbridge, Middlesex, UB8 3PH UK
[26]Nuclear Physics Department, Weizmann Institute of Science, Rehovot, 76100, Israel

[a]University of Victoria, Dept of Physics, P O Box 3055, Victoria BC V8W 3P6, Canada
[b]University of British Columbia, Dept of Physics, 6224 Agriculture Road, Vancouver BC V6T 1Z1, Canada
[c]Also at TRIUMF, Vancouver, Canada V6T 2A3
[d]On leave from Birmingham University, Birmingham B15 2TT, UK
[e]Univ of Victoria, Dept of Physics, P.O. Box 1700, Victoria BC V8W 2Y2, Canada and TRIUMF, Vancouver, Canada V6T 2A3
[f]Present address: Dipartimento di Fisica, Università della Calabria and INFN, 87036 Rende, Italy
[g]University of British Columbia, Dept of Physics, 6224 Agriculture Road, Vancouver BC V6T 2A6, Canada and IPP, McGill University, High Energy Physics Department, 3600 University Str, Montreal, Quebec H3A 2T8, Canada
[h]On leave from Research Institute for Computer Peripherals, Hangzhou, China
[i]On leave from Tel Aviv University, Tel Aviv, Israel

1 Introduction

An essential aspect of the Minimal Standard Model (MSM) of electroweak interactions [1] is the mechanism of spontaneous symmetry breaking by means of a Higgs doublet, which gives masses to the gauge particles $W^{\pm}$and Z^0, and to the fundamental fermions. However, the theory does not predict the masses of the Higgs bosons (H^0). In previous publications, OPAL [2] has excluded at the 95% confidence level (CL) a MSM Higgs boson with mass less than twice the muon mass (m_μ) and between 3 and 44 GeV/c^2 [3], while other LEP experiments have extended the excluded region to 48 GeV/c^2 [4]. Allowing for some model dependence in the decay of the Higgs boson, they have also excluded the intermediate mass region.

In this region between $2m_\mu$ and approximately 3 GeV/c^2, the models that have been used in previous searches to describe a MSM Higgs boson decay may not be accurate due to large QCD corrections to the $H^0 f\bar{f}$ vertex. These corrections involve the inclusion of "quark-triangle" graphs which lead to ambiguous results due to final state resonances [5]. Furthermore, the modelling of H^0 decays is incorrect if its mass overlaps with the scalar bound states of $c\bar{c}$ or $b\bar{b}$. In particular, searches based on large missing energy from the $e^+e^- \rightarrow Z^{0*}H^0, Z^{0*} \rightarrow \nu\bar{\nu}$ channel have relied on the correct modelling of charged and neutral decay modes of the H^0 in the intermediate mass region. The problems involved with correctly modelling the decays can be avoided by searching for all possible final states of the MSM H^0, which are clearly tagged by the decay $Z^{0*} \rightarrow \ell^+\ell^-$. A decay mode independent search sensitive to all kinematically accessible final states can also be used to set limits on the production of new scalar particles (S^0) which couple to the Z^0. Such a search is of interest for many supersymmetric extensions of the MSM [6] since they predict Higgs particles which have tree-level fermion couplings that are different from those of the MSM Higgs boson.

With 6.8 pb^{-1} of data recorded by the OPAL detector during the 1990 LEP run at CERN, a decay mode independent search is presented for the MSM H^0 in the mass region below 11.3 GeV/c^2, and includes an update to the search for Higgs bosons with mass below $2m_\mu$. Furthermore, the analysis is applied to search for any new scalars S^0 that couple to the Z^0.

A light Higgs boson can be produced at LEP via the process $Z^0 \rightarrow Z^{0*}H^0$. The searches presented here involve the decay:

$$Z^{0*} \rightarrow e^+e^- \text{ or } \mu^+\mu^-, \quad H^0 \rightarrow non{-}electromagnetic, \tag{1}$$

where the H^0 can decay into anything except final states containing only photons and/or an e^+e^- pair, and the complementary decay:

$$Z^{0*} \rightarrow \nu\bar{\nu}, \quad H^0 \rightarrow electromagnetic, \tag{2}$$

where the H^0 decays into states containing only photons and/or an e^+e^- pair.

Decays (1) and (2) are referred to throughout as the "charged lepton" and "neutrino" channels respectively. For centre-of-mass energies (E_{cm}) near 91 GeV, the Z^{0*} and H^0 recoil against each other with an average momentum of 7 GeV/c for $m_{H^0} \leq 3$ GeV/c^2, thus the

signature of decay (1) is that of inclusive acollinear lepton pairs. In the analysis for decay (1), a significant background arises from radiative dilepton processes, thus events with topologies consistent with $\ell^+\ell^-\gamma$, where the photon may or may not have converted, and $\ell^+\ell^-\gamma\gamma$ are rejected in the search. The charged lepton channel has sensitivity for nearly all H^0 decay modes; however, the removal of radiative backgrounds would reject long-lived Higgs bosons decaying into e^+e^- and Higgs bosons decaying purely into photons. These cases are recovered by the neutrino channel search, which are sensitive to precisely these decay modes of the Higgs boson. In decay (2), the events are characterized by large, isolated electromagnetic energy deposition and relatively few charged tracks.

Upper limits are given separately for the MSM Higgs boson production, where the Higgs boson lifetime is specified in terms of its mass, and for the production of new scalars where it is necessary to consider all kinematically available final states and lifetimes. For MSM Higgs bosons with masses in the range $0 \leq m_H \leq 2m_\mu$, the procedure discussed in a previous OPAL publication [2] is used. It considers only the decays $H^0 \to e^+e^-$ and $H^0 \to \gamma\gamma$, and includes non-vanishing lifetimes of the H^0 due to the smaller value of the $H^0 f\bar{f}$ coupling. The neutrino channel search is used for cases where the H^0 is short-lived and therefore its decay products would deposit energy in the electromagnetic calorimeter. In the case where the MSM H^0 decays outside the detector, only the charged lepton search channel is used, since the $Z^{0*} \to \ell^+\ell^-$ decays would trigger the detector. In the mass range $m_H \geq 2m_\mu$, where more complicated final states are accessible to the MSM H^0 decay, the efficiency is evaluated for any possible MSM H^0 final state. Efficiencies for the detection of new scalars S^0 are calculated using no specific decay model, allowing for decays into all kinematically accessible final states and lifetimes, including decays to undetected particles. The search results are then combined to obtain limits on the production rate as a function of mass.

2 The OPAL Detector

The measurements reported here made use of the OPAL detector [7], which is a multipurpose apparatus having nearly 4π steradians acceptance. The central detector (CD) consists of a system of tracking chambers inside a 0.435 T solenoidal magnetic volume. The CD system is surrounded by a time-of-flight (TOF) counter array, a lead glass electromagnetic calorimeter (EM) with a presampler, an instrumented magnet return yoke serving as a hadron calorimeter (HC), muon chambers (MU), and an endcap system which includes a low-angle forward detector (FD). The analysis presented here relied mostly on the EM, CD, MU, and FD systems. Cosmic ray rejection made use of the TOF, HC, and MU systems.

The central tracking detector consists of a precision vertex chamber surrounding a beam-pipe of approximately 8 cm radius, a large volume "jet" chamber (CJ), and a chamber for tracking in the $r-\theta$ plane (the coordinate system is defined with $+z$ along the e^- beam, θ and ϕ being the polar and azimuthal angles, respectively). The tracking, momentum measurement, and ionization energy loss (dE/dx) measurements of charged particles are performed with the CJ, a drift chamber approximately 4 metres in length and 2 metres radius, with 24 sectors in

ϕ and 159 layers of sense-wires in each sector. Tracks having $|\cos\theta| \leq 0.97$ traverse at least 20 space points in the jet chamber. The TOF system covers the barrel region of $|\cos\theta| \leq 0.82$ and consists of 160 scintillator bars, 6.8 m long and 45 mm thick, located at a radius of 2.4 m.

The EM consists of a cylindrical array of 9440 lead glass blocks of 24.6 radiation lengths thickness in the barrel region (EB) covering the range $|\cos\theta| < 0.82$, and 2264 lead glass blocks of 20 radiation lengths thickness in the endcap (EE) region covering the range $0.81 < |\cos\theta| < 0.98$. Each block subtends a solid angle of approximately 40×40 mrad^2 and projects towards a point near the interaction point in the barrel region and along the beam direction in the endcaps. The two sections of the EM cover 98% of the solid angle.

The hadron calorimeter consists several layers of 10 cm iron plates, which results in a total thickness greater than 4.7 interaction lengths for 97% of 4π, interspersed with layers of limited-streamer tubes having both pad and strip readout. It is used in this analysis to identify nonelectromagnetic showers and cosmic rays, and information from the strips is used in conjunction with the muon chambers for muon identification. The muon detector consists of 4 layers of drift chambers (barrel region) or limited-streamer chambers (endcaps) which are shielded by a minimum of 1.3 m of iron. In this analysis, muons are associated with "segments", which are defined by triplets of hits in the MU or HC.

The luminosity of the colliding beams was determined by observing small angle Bhabha scattering with the forward detector, a lead/scintillator calorimeter with associated tracking chambers, at either end of the central detector, with an acceptance covering $40 < \theta < 150$ mrad and 2π in azimuth. This device achieves an accuracy of better than 1% in the luminosity measurement [8].

Tracks and clusters were selected for use in this study if they met the following requirements. Tracks were required to have at least 20 hits and no less than 50% of the geometrically possible number of hits in the CJ, and a momentum transverse to the beam axis (p_t) exceeding 0.150 GeV/c. Their distances-of-closest-approach to the origin in the plane perpendicular to ($|d_0|$) and parallel to the beam ($|z_0|$) had to be less than 2.5 cm and 50.0 cm, respectively. EM clusters in the barrel were selected if they had energies greater than 0.17 GeV, and clusters in the endcap were selected if they had energies greater than 0.25 GeV and contained at least 2 lead glass blocks.

To ensure the correct measurement of charged tracks, electromagtic energy, and luminosity events, subdetectors important to the analysis were required to have fully operational status. Subdetector status requirements differ slightly between the charged lepton and neutrino channel analysis. The data satisfying these requirements represent integrated luminosities of 6.8 and 6.0 pb^{-1} for the charged lepton and neutrino channels, respectively. These integrated luminosities are listed in table 1.

3 The Monte Carlo Simulation

The MSM Higgs boson cross section was calculated using the Berends and Kleiss Born generator [9] which incorporates first order QED corrections. The coupling constants were calculated using the Improved Born approximation [10] with $m_Z = 91.15$ GeV/c^2 and the corresponding Standard Model value for Γ_Z, while taking into account the effective electroweak couplings $\alpha(Q^2)$ and $\sin^2\bar{\theta}_W$ at the Z^0 mass. The effects of higher order initial state radiation (ISR) were calculated using the exponentiation technique of Nicrosini and Trentadue [12]. The overall theoretical uncertainty for the Higgs boson production cross section obtained in this manner is estimated to be less than 2%.

The OPAL detector response to the generated particles was modelled using a simulation program [13] based on the GEANT [14] package, which provides a detailed description of the response of the various detector components to the passage of particles.

Because of the complementary nature of the charged lepton and neutrino analyses, accurate modelling of the specific H^0 final states is not important. For the neutral decay modes, the $\gamma\gamma$ and $\pi^0\pi^0$ final states have been used to calculate the efficiency. The low-mass Higgs boson momentum spectrum is sensitive to E_{cm}, and therefore the analyses have E_{cm} dependent correction factors. Furthermore, the efficiency to detect long-lived Higgs bosons must also account for the momentum dependence of the decay lengths. Efficiencies were determined using simulations that included first order radiative corrections, and the effect of higher order corrections was estimated to introduce an error of less than 1% in the efficiency of the searches described. The corrections are listed in table 1.

4 Charged Lepton Channel Search

The decay $Z^0 \to Z^{0*}H^0$, $Z^{0*} \to e^+e^-$, or $\mu^+\mu^-$ can be tagged by identifying an acollinear, high-momentum lepton pair. Candidate lepton tracks were taken as the two highest momentum CD tracks (p_1 and p_2) in the event. For this channel, an EM cluster was associated to the candidate lepton track if it was the nearest one lying within 15° of the track.

To select electrons, the candidate lepton tracks were required to satisfy all of the following conditions:

- the two tracks were required to have $p_1 \geq 25$ GeV/c and $p_2 \geq 15$ GeV/c. This unequal momentum requirement increases sensitivity to asymmetric $Z^{0*} \to \ell^+\ell^-$ decays;
- all the electromagnetic energy in a 15° half-angle cone about p_1 was required to be at least 30 GeV, and similarly, 20 GeV for p_2;
- the two tracks were required to have $|\cos\theta| \leq 0.7$. This requirement rejects events with electrons entering a region of the EM preceded by a large amount of material which

degrades the energy resolution. In addition, this requirement removes background from t-channel processes.

To select muons, the candidate lepton tracks were required to satisfy all of the following conditions:

- $p_1 \geq 30$ GeV/c and $p_2 \geq 20$ GeV/c;
- the two tracks were associated with segments in the MU or HC detectors;
- both tracks satisfied $|\cos\theta| \leq 0.9$.

The p_1, p_2 momentum requirements for the electron pair were less severe than that for the muon pair in order to be less sensitive to the simulation of final state radiation. With the above cuts, 4851 electron and 6021 muon pair candidates were selected. In Monte Carlo simulations of $Z^0 \rightarrow (e^+e^-, \mu^+\mu^-)$, using BABAMC [16] and KORALZ [15], electron and muon pair events in the detector acceptance region were selected with efficiencies of 0.996 ± 0.013 and 0.930 ± 0.020 respectively. Systematic differences in the efficiency and acceptance between detector simulation and data have been studied and estimated to be less than 2%. The trigger efficiency for these events is effectively 100%. After these cuts, the expected backgrounds from $Z^0 \rightarrow \tau^+\tau^-$ and $Z^0 \rightarrow q\bar{q}$ were estimated using the KORALZ and Jetset 7.2 [17] Monte Carlos, contributing 76.7 and 58.4 events, respectively.

Since the Higgs boson would be produced with a large momentum recoiling against the Z^{0*}, the events can be selected efficiently by searching for acollinear lepton tracks. However, in order to be less sensitive to background from $Z^0 \rightarrow \ell^+\ell^-$ with hard ISR, the acollinearity requirement is made on acoplanarity. The acoplanarity angle ϕ_{acop} between the leptons is defined as $\pi - \phi_{open}$, where ϕ_{open} is the azimuthal opening angle between their momenta. Each momentum vector used to calculate ϕ_{acop} was formed by vectorially summing the primary track momenta together with any unassociated electromagnetic energy within 15° to include possible final state radiation. An acollinearity requirement was then made on the "weighted acoplanarity" α defined as:

$$\alpha \equiv \phi_{acop} < \sin\theta >$$

where $< \sin\theta >$ is the average of the absolute values of the sine of the lepton track polar angles. Weighting the acoplanarity in this manner takes into account the acoplanarity which results from configurations where the acollinear track pairs have small polar angles to the beam axis. The quantity is a function solely of the H^0 and E_{cm} since it only depends on approximately the p_t recoiling against the tracks. The quantity α was required to satisfy $0.1 \leq \alpha \leq 2.88$ rad; the upper value of the cut ensured that the 15° lepton cones did not overlap. Figure 1 shows the α distribution for the data, for a simulation of $Z^0 \rightarrow \ell^+\ell^-$ decays, and for a simulation of $Z^0 \rightarrow Z^{0*}H^0$, $Z^{0*} \rightarrow \ell^+\ell^-$ for a 3 GeV/c^2 Higgs boson.

4.1 Rejection of Radiative Dilepton and Multihadrons

After imposing the requirements mentioned above to select an acoplanar topology, the charged lepton channel analysis remains sensitive to any Higgs boson decay mode since these requirements concern only the lepton tracks. The remaining event sample is mostly $Z^0 \to \ell^+\ell^-$ events containing radiative photons (which may or may not have converted), and some background from multihadronic events. Events containing one or two EM clusters not associated with the primary leptons were therefore rejected if all the following requirements were met:

- there were one or two EM clusters outside of the 15° lepton cones, with the clusters being consistent with electromagnetic energy deposition (their energy exceeded 1 GeV, and there was less than 2 GeV of HC energy associated to them);
- there were no tracks outside of the 15° lepton cones;
- the total electromagnetic energy outside of the 15° lepton cones was larger than 4 GeV.

The 4 GeV electromagnetic energy requirement was imposed in order to match the energy requirement used in the neutrino channel analysis (section 5). The total electromagnetic energy unassociated to the lepton tracks for events removed by the requirements above is shown in figure 2 for data, and for Monte Carlo simulation of $Z^0 \to \ell^+\ell^-(\gamma)$.

Events were also rejected as being $\ell^+\ell^-\gamma(\gamma)$ events with one of the photons converting if the events contained exactly 2 tracks more than 15° from the primary leptons, and a conversion vertex was identified at a radius larger than 7 cm. This radius cut value was chosen in order to reject conversions occuring in the beam-pipe, which has approximately 8 cm radius. In order to avoid rejection of Higgs bosons with a mass near a two-particle threshold, events were rejected only if one of the conversion tracks had p_t less than 2 GeV/c. Such two-prong decays of the H^0 would resemble stiff, symmetric conversion pairs whose small curvature introduces a large uncertainty in the reconstructed vertex position. A study of conversions in multihadronic decays of the Z^0 has shown that the vertex radius is reconstructed with an error of 1.4 cm when one track has p_t less than 2 GeV/c. Since the conversion cut rejects tracks with vertices more than 5 standard deviations from the event origin, it has a negligible effect on a hypothetical short-lived Higgs boson signal.

Events consistent with being multihadronic decays of the Z^0 were removed if the invariant mass of the event (excluding the leptons) was larger than 20 GeV/c^2. The value of the cut was chosen in order to reject only events with mass values far above the search mass range of 11.3 GeV/c^2; therefore, the inefficiency introduced by the cut for $m_{H^0} \leq 11.3$ GeV/c^2 is small. The invariant mass was calculated using the algorithm discussed in a previous OPAL publication [3], which takes into account double counting of track momenta and calorimeter energy. Only tracks and clusters that were more than 15° away from the lepton tracks were used in the algorithm. To determine the efficiency loss due to this procedure, two extreme cases were studied for decays of a 12 GeV/c^2 Higgs boson, namely decay into a $\pi^+\pi^-$ final state, as well as a MSM Higgs boson coupling into quarks and leptons, where the quarks were

fragmented using the Jetset 6.3 Monte Carlo [17] default. The mass requirement introduced a 2.3% inefficiency. The cut removes three events, leaving a total of five candidate events.

4.2 Final Event Sample

Table 2 shows the number of events surviving after each cut for the data and the various Monte Carlo generators. Five events remain as candidates after all cuts. One event is consistent with being a conversion. The two non-lepton tracks in the event have an invariant mass of 0.38 GeV/c^2 and form a conversion-type vertex with radius larger than 7 cm, but it survives the conversion removal cut since the p_t of the tracks are slightly larger than 2 GeV/c. Three events are consistent with being background events from four-fermion final states. They have invariant masses of 0.75 GeV/c^2, 0.74 GeV/c^2, and 0.12 GeV/c^2. The remaining event has two tracks in addition to the lepton tracks, and a single unassociated energetic EM cluster. The tracks have momenta of 0.60 GeV/c and 0.71 GeV/c, and the EM cluster has an energy of 25.6 GeV. The invariant mass of this combination of tracks and cluster is 10.0 GeV/c^2. In these measurements, the particles have been assumed to be massless.

The dominant background to the search in the charged lepton channel consists of stiff conversions from radiative lepton pairs, and four-fermion final states [11]. The latter has been modelled by a Monte Carlo that generates, using the lowest-order calculation, final states with four leptons, including diagrams involving both weak and electromagnetic interactions [19]. Since most of the four-fermion events in the background are four-fermion decays of the Z^0, their rate would be influenced by ISR corrections which are not modelled in this Monte Carlo. Using an analytical formula [20], a correction factor for ISR was calculated which takes into account the E_{cm} scan. It is given by the luminosity-weighted ratio $\sigma(Z^0 \rightarrow q\bar{q}$ with ISR$)/\sigma(Z^0 \rightarrow q\bar{q}$ without ISR), which yields the value 0.85. This correction is not valid for the emission of $f\bar{f}$ pairs from the initial state, which contributes between 8% at the Z^0 peak to 16% at $E_{cm} = 94$ GeV for the analysis presented here. Taking these contributions into account, a 15% systematic error has been assigned to the use of the correction. The predicted rate for $\ell^+\ell^- q\bar{q}$ was also estimated from the Monte Carlo [19]. Assuming that lepton pairs of the four-lepton final state come from a single virtual photon emission, the rate for $q\bar{q}$ emission was estimated to be the rate for lepton pair emission scaled by the R-value measured in lower energy e^+e^- annihilations [21] and evaluated at the lepton pair invariant mass. The total number of four-fermion events expected in the data is 3.3 ± 0.4 events.

As a consistency check, the data for the four-fermion final states was compared to the Monte Carlo [19] at a more significant level by loosening the cuts for the charged lepton channel. The weighted acoplanarity requirement was dropped, and the primary lepton tracks were required to have $|\cos\theta| \leq 0.9$, and momenta p_1 and p_2 exceeding only 10 GeV/c. No lepton identification was applied in order to be sensitive to tracks that are from $\tau^+\tau^-$ decays. A requirement on the isolation of the primary lepton tracks, which is used only in this consistency check, was applied in order to remove background from multihadrons and $\tau^+\tau^-$. This cut required events to have no other tracks within the 15° lepton cones. After these cuts, 26 events remain which compares favorably with 21.1±2.4 events predicted by the Monte Carlo, plus 4±2 events predicted by

the Jetset 7.2 Monte Carlo [17] for the $Z^0 \to q\bar{q}$ background. Finally, the primary tracks in the events were classified as e^+e^- or $\mu^+\mu^-$ based on track association with segments in the MU or HC for muons, or $E_1/p_1, E_2/p_2 \geq 0.7$ for electrons. Primary tracks not satisfying the requirements were classified as $\tau^+\tau^-$. As shown in table 4, the expected contributions for each of the classifications also agree well with the data.

The remaining background from conversions is estimated from Monte Carlo simulation of $Z^0 \to e^+e^-(\gamma)$, $\mu^+\mu^-(\gamma)$, where the accuracy depends on the material description in the detector simulation. The conversion rate has been checked using the process $e^+e^- \to \gamma\gamma$, and the Monte Carlo agrees with the data within the statistical error (20%). This conversion background contributes an expected 1.8 ± 1.1 events, while background from $Z^0 \to q\bar{q}$, $\tau^+\tau^-$ contributes 1.2 ± 1.1 events. Therefore, the total expected background is 6.3 ± 1.6 events.

The overall efficiencies, after all the charged lepton channel cuts, are listed in table 3. The OPAL trigger is effectively 100% efficient for these events. Based on studies of $Z^0 \to e^+e^-, \mu^+\mu^-$ decays, the lepton identification requirements contribute a 2% systematic error on the efficiency, and the requirements on p_1 and p_2 contribute another 2% systematic error. Monte Carlo statistics contribute an additional 6% uncertainty.

Throughout most of the H^0 mass range for the MSM H^0 search, the five remaining events are accepted as candidates. However, in the particular case of the range $m_H \leq 2m_\mu$ where $H^0 \to (e^+e^-$ or $\gamma\gamma)$, the charged lepton channel analysis is designed to be only sensitive to Higgs bosons decaying *outside* the detector. Therefore, the search for MSM H^0 in this region has an additional cut demanding no other activity in the detector; the remaining events are required to have no tracks outside the 15° lepton cones, and no other EM clusters above 1 GeV in energy. None of the five remaining events satisfy this requirement.

5 Neutrino Search Channel

The decays $Z^{0*} \to \nu\bar{\nu}$, with the Higgs boson decaying inside the detector to e^+e^- and/or states containing photons, are identifiable as having an isolated region of the detector containing only electromagnetic energy. They trigger the OPAL detector on the basis of their electromagnetic energy deposition with better than 98.7% efficiency if at least 1.5 GeV of energy is deposited in the EB and an electromagnetic shower originates in the coil to fire a signal in the TOF [18]. The principle selection criterion for the final states of the H^0 in this channel consists of requiring large deposited electromagnetic energy; it is designed to be sensitive to Higgs events of the type which are removed by the $\ell^+\ell^-\gamma$, $\ell^+\ell^-\gamma\gamma$, and conversion vetos used in the charged lepton channel search (see section 4). Events were selected if they satisfied all the following criteria:

- at least 4 GeV was deposited in the barrel EM;
- the energy-weighted vector sum of all EM clusters, $\vec{E}$, satisfied $|\cos\theta_{\vec{E}}| < 0.70$;

- there were either no tracks having at least 20 hits in the CJ, or at least two such tracks. The latter enables this analysis to maintain sensitivity to H^0 decays into e^+e^-.

In order to remove background from $e^+e^- \to \gamma\gamma(\gamma)$ and $Z^0 \to \ell^+\ell^-$, events were required to have a visible mass to be less than 20 GeV/c^2 and no good tracks, as defined in section 2.1, more than 45° away from $\vec{E}$. Backgrounds from low Q^2 radiative Bhabha events and two-photon events which deposit energy mainly in the forward direction were removed by requiring that there be less than 2 GeV deposited in the FD subdetector, and no more than half the total electromagnetic energy deposited in the EE subdetector.

Cosmic ray muons and beam halo particle backgrounds are characterized by cluster shapes in the EM, signals in the HB and/or MU, and 'out-of-time' signals in the TOF counter. Therefore, events were required to satisfy all of the following additional criteria:

- there was a TOF counter hit within 200 mrad in azimuth of an EM cluster;
- the mean TOF time was less than 1.1 ns (three standard deviations) from that expected for a particle coming from the interaction point;
- no muon chamber segments were present;
- no more than 4 GeV energy was deposited in the hadron calorimeter;
- no more than 3 strip hits within a 45° ϕ wedge in the outer 8 layers of the hadron barrel calorimeter were present;
- all the EM clusters had a width in ϕ and θ of less than 0.25 rad.

After applying all the above requirements, 17 events remain. Of these, 16 events are consistent with being $e^+e^- \to \nu\bar{\nu}\gamma$, 4 of which have the photon converting in the material near the interaction region. The remaining event has a mass of 3.2 GeV/c^2 and is a poorly measured, acollinear but coplanar event consistent with the topology expected from two-photon processes.

The dominant background in the neutrino channel search comes from the process $e^+e^- \to \nu\bar{\nu}\gamma$. The Monte Carlo used to simulate this process [22] has been shown to reproduce well the spectra of low energy photons in the data [18]. Its prediction for the background surviving the 4 GeV minimum barrel EM energy cut is 12.1±1.1 events, in reasonable agreement with the value seen remaining in the data. Other additional backgrounds surviving the 4 GeV minimum barrel EM energy cut are small. The barrel electromagnetic energy distribution for the data is shown in figure 3, along with the expected distribution from the $e^+e^- \to \nu\bar{\nu}\gamma$ background. The distribution expected for a hypothetical Higgs boson of mass 1 GeV/c^2 decaying entirely to $\pi^0\pi^0$ is superimposed on the figure. Also indicated is the 4 GeV barrel EM energy cut, which removes a significant portion of the $e^+e^- \to \nu\bar{\nu}\gamma$ background while retaining a high signal sensitivity.

The efficiency of the neutrino channel analysis is essentially independent of the particular neutral final state. For the efficiency calculation, $\gamma\gamma$ and $\pi^0\pi^0$ final states were used. Some loss

of efficiency arose from the presence of spurious signals in the detector. This was estimated by measuring the occupancy in the various subdetectors in random beam crossing events. Based on these studies, an inefficiency of 1.18±0.04% is attributed to effects of detector noise arising from the various vetos used in the analysis. An inefficiency of 0.4±0.1% was introduced by the TOF requirement as determined using single electron events arising from the processes $e^+e^- \rightarrow e^+e^-\gamma$ and $e^+e^- \rightarrow e^+e^-e^+e^-$, where the visible electron track satisfies $|\cos\theta| < 0.7$. The combined efficiency arising from these various measured detector effects is $(98.4 \pm 0.1\%)$. For the decays $H^0 \rightarrow \pi^0\pi^0$ or $\gamma\gamma$, the TOF requirement introduces an additional efficiency loss, modelled in the Monte Carlo, since the cut requires a photon to convert in the coil.

The overall selection efficiency after the cuts above is indicated in table 3. The contributions to the systematic error on the efficiencies arise from the simulation of detector response (5.0%), the Monte Carlo statistics (3.5%). Other sources of error, due to the inefficiency introduced by detetector-related effects, contribute less than 0.1%.

The neutrino search channel is also sensitive to new scalar particles S^0 that couple to the Z^0, and therefore is designed to have sensitivity to all kinematically accessible final states including those that contain long-lived particles. Therefore, no additional cuts were applied, and the 17 remaining events are accepted as candidates. For the MSM H^0 search, where the H^0 mass is greater than $2m_\mu$ and is short-lived, an additional cut was applied which required the events to have a visible mass greater than 1 GeV/c^2. One event survives after this cut. The small remaining background surviving this mass cut arises from two-photon processes and its estimation is uncertain; therefore, it is not considered in the neutrino channel analysis. Since the cut makes the analysis inefficient to Higgs bosons of small mass, only the upper limits for a MSM H^0 with mass greater than 3 GeV/c^2 were evaluated using the cut. For $H^0 \rightarrow \pi^0\pi^0$, this additional mass requirement introduces a 10% inefficiency for $m_H \geq 3$ GeV/c^2.

6 Expected Number of Higgs Bosons and Combined Limits

In this section, upper limits are given separately for MSM Higgs boson production, where there is a known lifetime as a function of the mass, and for the production of new scalars, where it is necessary to consider all kinematically available final states. In the latter case, the particle lifetime is not specified, so a worst-case lifetime is used in obtaining limits on particle production. A summary of the data passing the cuts and the expected backgrounds for the MSM H^0 analysis mode is given in table 5. In quoting the limits, efficiency and acceptance variations due to subdetector requirements and E_{cm} dependence are accounted for. The integrated luminosities used in each search channel and the number of expected MSM Higgs bosons produced are listed in table 1. The total systematic uncertainties in the efficiency calculations are 6.6% and 6.1% for the charged lepton and neutrino channel, respectively. The theoretical uncertainty in MSM Higgs boson production is 2%, and the luminosity systematic error is 1.0%. Therefore, the final uncertainties in the number of Higgs bosons are 7.0% and 6.5% for the charged lepton and neutrino channels, respectively. To be conservative in giving

the limit, the values used for the expected number of Higgs bosons were reduced by the above errors, and the estimated background levels were reduced by one standard deviation in their systematic uncertainties. The technique of the Particle Data Group [23] is used to calculate 95% confidence level (CL) upper limits for a possible signal; this procedure is valid for the Poisson distributed statistics of the background.

In the MSM H^0 search where $m_H \leq 2m_\mu$, the search is performed only for the decay $H^0 \to (e^+e^-$ or $\gamma\gamma)$ while taking into account effects due to the non-negligible lifetime of the Higgs boson. In the case where the H^0 decays outside the detector, the detection efficiency is evaluated using only the charged lepton channel where the $Z^{0*} \to \ell^+\ell^-$ decays would trigger the detector. For short-lived H^0, the e^+e^- or $\gamma\gamma$ final states will deposit energy in the EM, and thus are visible in the neutrino channel. Thus, while there are only the e^+e^- and $\gamma\gamma$ final states in this mass region, the combination of the charged lepton and neutrino search channels is sensitive to all lifetimes. The expected number of events in each channel and the combined total are shown figure 4a. Also shown in the figure is the (mass-dependent) 95% CL upper limit (henceforth referred to simply as "upper limit") which accounts for the observation of 17 events in the neutrino channel and 0 events in the charged lepton channel. The expected number of events is much larger than the upper limit on the number of observed events throughout this mass region.

For a MSM H^0 with mass larger than $2m_\mu$, more complicated final states are possible. In the charged lepton channel, 5 events are observed, compared to a predicted background of 6.3 ± 1.6 events. Together with reducing the expected background by one standard deviation, the 95 % CL upper limit is 6.5 events. For the neutrino channel, 17 events are observed, compared to a predicted background of 12.2 ± 1.1 events, giving an upper limit of 14.4 events. For the region $m_H \geq 3$ GeV/c^2, the analysis requires the visible mass to exceed 1 GeV/c^2. In this region there is 1 event observed, giving an upper limit of 4.7 events. The efficiency for the neutrino channel was determined using the modes $H^0 \to \pi^0\pi^0$ and $\gamma\gamma$, and it was assumed to be the same for all the neutral modes. The numbers of expected events for the two channels, *assuming a 100% H^0 branching ratio into each channel*, and the upper limits for signal, are shown in figure 4b.

In obtaining limits for new scalars, the same procedure as described above was used for the search in the region $m_S \geq 2m_\mu$, except that the 1 GeV/c^2 visible mass cut was not applied to the 17 events in the neutrino channel in order to retain sensitivity to all kinematically accessible final states, including long-lived ones. For the $m_S < 2m_\mu$ region, no model is assumed for the S^0 lifetime, so the worst-case lifetime is taken from the MSM analysis.

Figure 5a shows the upper limit on the H^0 production rate, relative to the MSM value, including the MSM H^0 lifetime dependence on m_{H^0}. For $m_{H^0} < 2m_\mu$, the limit is obtained by dividing the upper limit for signal in the *combined* search channels by the expected number. For the $m_{H^0} > 2m_\mu$ region, a mass-dependent upper limit on Higgs boson production cross section is obtained by adding the ratios

$$R^i = \frac{N^i_{95}}{N^i_{max}}, \tag{3}$$

for the two complementary search channels i. In (3), N_{95} is the upper limit for a signal, and N_{max} is the expected number of events, *assuming a 100% branching fraction into the given search channel.* Owing to the complementary nature of the charged lepton and neutrino channel searches, this procedure gives the most pessimistic total production rate. Figure 5a shows that a MSM H^0 is excluded for any possible decay mode up to a mass of 11.3 GeV/c^2.

Figure 5b shows the limits on S^0 production, relative to the MSM H^0 production, when no assumption is made about the lifetime-versus-mass relation of the scalar particle (i.e., no minimum mass cut is applied to the scalar system). The figure indicates that any scalar particle produced in conjuction with a Z^{0*} is excluded up to a mass of 9.5 GeV/c^2 if its coupling to Z^0Z^{0*} is that of the MSM Higgs boson. Finally, since the present search is independent of the charged multiplicity of the decay products, it can be used to set limits on the production of the lightest Higgs boson (h^0) of the Minimal Supersymmetric Standard Model and other models containing more than one Higgs doublet [6]. In particular, in some regions of the coupling parameters, the decay $h^0 \rightarrow \tau^+\tau^-$ would be dominant. In this case, the limit on h^0 production can be given solely by the search in the charged lepton channel and is indicated in figure 5b by the dashed line.

7 Conclusions

Using OPAL data from the 1990 LEP run, searches for $e^+e^- \rightarrow Z^{0*}H^0$, where $Z^{0*} \rightarrow e^+e^-$, $\mu^+\mu^-$, or $\nu\bar{\nu}$, and the H^0 decaying arbitrarily have been performed. The existence of any scalar particle produced in conjunction with a Z^{0*} with MSM strength is excluded at 95% CL in the mass range $0 \leq m_S \leq 9.5$ GeV/c^2, with no assumptions made about the scalar decay mode. Furthermore, if one assumes the MSM mass-lifetime relationship, the limit covers the region $0 \leq m_H \leq 11.3$ GeV/c^2. Combining the results of this publication with that described in previous searches for a Higgs boson [3, 24], OPAL has excluded a Minimal Standard Model Higgs boson unambiguously in the mass range $0 \leq m_H \leq 44$ GeV/c^2.

8 Acknowledgements

It is a pleasure to thank the SL Division for the efficient operation of the LEP accelerator, the precise information on the absolute energy, and their continuing close cooperation with our experimental group. In addition to the support staff at our own institutions we are pleased to acknowledge the following :
Department of Energy, USA;
National Science Foundation, USA;
Science and Engineering Research Council, UK;
Natural Sciences and Engineering Research Council,Canada;
Israeli Ministry of Science;
Minerva Gesellschaft;

The Japanese Ministry of Education, Science and Culture (the Monbusho) and a grant under the Monbusho International Science Research Program;
American Israeli Bi-national Science Foundation;
Direction des Sciences de la Matière du Commissariat à l'Energie Atomique, France;
The Bundesministerium für Forschung und Technologie, FRG; and
The A.P. Sloan Foundation.

References

[1] S. L. Glashow, J. Iliopoulous and L. Maiani, Phys. Rev. **D2** (1970) 1285;
S. Weinberg, Phys. Rev Lett. **19** (1967) 1264;
A. Salam, Elementary Particle Theory, ed. N. Svartholm (Almquist and Wiksells, Stockholm, 1969), p. 367;
P. W. Higgs, Phys. Rev. Lett. **12** (1964) 132;
F. Englert and R. Brout, Phys. Rev. Lett. **13** (1964) 321.

[2] OPAL Collab., M. Z. Akrawy *et al.*, Phys. Lett. **B251** (1990) 211-222.

[3] OPAL Collab., M. Z. Akrawy *et al.*, Phys. Lett. **B253** (1991) 511-523;
OPAL Collab., M. Z. Akrawy *et al.*, Phys. Lett. **B236** (1990) 224.

[4] ALEPH Collab., D. Decamp *et al.*, CERN-PPE/91-19 (1991);
ALEPH Collab., D. Decamp *et al.*, Phys. Lett. **246B** (1990) 306-314;
ALEPH Collab., D. Decamp *et al.*, Phys. Lett. **245B** (1990) 541;
ALEPH Collab., D. Decamp *et al.*, Phys. Lett. **241B** (1990) 141-149;
ALEPH Collab., D. Decamp *et al.*, Phys. Lett. **236B** (1990) 233-244;
ALEPH Collab., D. Decamp *et al.*, Phys. Lett. **235B** (1990) 399-411;
DELPHI Collab., P. Abreu *et al.*, CERN-PPE/90-193 (1990);
DELPHI Collab., P. Abreu *et al.*, CERN-PPE/90-163 (1990);
DELPHI Collab., P. Abreu *et al.*, Nucl. Phys. **B342** (1990) 1;
DELPHI Collab., P. Abreu *et al.*, Phys. Lett. **B245** (1990) 246;
L3 Collab., B. Adeva *et al.*, L3 preprint #24, December 1990;
L3 Collab., B. Adeva *et al.*, L3 preprint #19, September 1990;
L3 Collab., B. Adeva *et al.*, L3 preprint #15, August 1990;
L3 Collab., B. Adeva *et al.*, L3 preprint #10, June 1990.

[5] J.Ellis, M.K.Gaillard and D.V.Nanopoulos, Nucl. Phys **B106** (1976) 292;
M.Voloshin and V.Zakharov, Phys. Rev. Lett. **45** (1980) 688;
M.Voloshin, Sov. J. Phys. **44** (1986) 478;
S.Raby and G.B.West, Phys. Rev. **D38** (1988) 3488.

[6] P. J. Franzini and P. Taxil, *Z Physics at LEP* 1, CERN 89-08 (1989), ed. G. Altarelli *et al.*, Volume 2, 91;
S. Dawson, J. F. Gunion, H. E. Haber, G. L. Kane, *The Higgs Hunter's Guide*, **BNL**-41644 (1989), Submitted to Physics Rep.

[7] OPAL Collab., K. Ahmet *et al.*, CERN-PPE/90-114 (1990)
(Submitted to Nucl. Instr. and Meth.).

[8] OPAL Collab., M. Akrawy *et al.*, CERN-PPE/91-67 (1991).

[9] F. A. Berends and R. Kleiss, Nucl. Phys. **B260** (1985) 32.

[10] M. Consoli and W. Hollik, *Z Physics at LEP* 1, CERN 89-08 (1989), ed. G. Altarelli *et al.*, Volume 1, 39;
G. Burgers, W. Hollik, Polarization at LEP (1988), Volume 1, 136.

[11] E. W. N. Glover and J. J. van der Bij, *Z Physics at LEP* 1, CERN 89-08 (1989), ed. G. Altarelli *et al.*, Volume 2, 11.

[12] O. Nicrosini and L. Trentadue, Phys. Lett. **B196** (1987) 551.

[13] J. Allison *et al.*, Computer Physics Communications **47** (1987) 55.

[14] R. Brun, F. Bruyant, M. Maire, A. C. McPherson, and P. Zanarini, *GEANT*3, CERN DD/EE/84-1 (1987).

[15] S. Jadach, B. F. L. Ward, Z. Was, R. G. S. Stuart, and W. Hollik, KORALZ *The Monte Carlo Program for* τ *and* μ *pair Production Processes at* LEP/SLC, unpublished (1989).

[16] M. Bohm, A. Denner and W. Hollik, Nucl. Phys. **B304** (1988) 687;
F. A. Berends, R. Kleiss, and W. Hollik, Nucl. Phys. **B304** (1988) 712.

[17] T. Sjöstrand, Comp. Phys. Comm. **39** (1986) 347;
T. Sjöstrand and M. Bengtsson, Comp. Phys. Comm. **43** (1987) 367.

[18] OPAL Collab., M. Z. Akrawy *et al.*, CERN-PPE/90-187 (1990)
(Submitted to Zeit. fuer Phys. C).

[19] F.A.Berends, P.H.Daverveldt and R.Kleiss, Nucl. Phys. **B253** (1985) 421;
Private Communication with J. Hilgart and R. Kleiss.

[20] F. A. Berends, R. Kleiss and S. Jadach, Comp. Phys. Commun. **29** (1983) 185.

[21] In the region $E_{cm} < 1$ GeV, R-values are taken from L. M. Barkov *et. al.*, Nucl. Phys. **B256** (1985) 365;
R-values for higher E_{cm} are the values quoted in the review article by H. Burkhardt, F. Jegerlehner, G. Penso, and C. Verzegnassi, *Polarization at LEP*, CERN 88-08 (1988), Vol. 1, 145;
K. J. Abraham and J. J. van der Bij, Phys. Lett. **248B** (1990) 199;
L. Bergström and R. W. Robinett, Phys. Lett. **245B** (1990) 249.

[22] R. Miquel, C. Mana, and M. Martinez, Zeit. fuer Phys. **C48** (1990) 309;
F. A. Berends, G. Burgers, C. Mana, M. Martinez, and W. L. van Neerven, Nucl. Phys. **B301** (1988) 583.

[23] P.D.G. Review of Particle Properties, Phys. Lett. **B239** (1990) III.35.

[24] OPAL Collab., M. Z. Akrawy *et al.*, Zeit. fuer Phys. **C49** (1991) 49-57.

Tables

Table 1: Cross section for $e^+e^- \to Z^{0*}H^0$ for a 1 GeV/c^2 Higgs boson and integrated luminosities of the data as a function of E_{cm}. ϵ_{rel} is the efficiency relative to the peak for the selection procedures. Luminosity differences between search channels arise from different detector operational status requirements used in the analyses. The overall systematic error is 20 MeV on the energy scale and 1.0% on the luminosity.

Centre-of-Mass Energy (GeV)	Cross section for $e^+e^- \to Z^{0*}H^0$ (nb)	Relative Efficiency ϵ_{rel}	Luminosity (nb^{-1})		
			$Z^{0*} \to e^+e^-$	$Z^{0*} \to \mu^+\mu^-$	$Z^{0*} \to \nu\bar{\nu}$
88.25	0.025	1.14	502	496	470
89.25	0.056	1.13	658	652	433
90.25	0.153	1.08	354	345	327
91.25	0.333	1.00	3628	3571	3195
92.25	0.323	0.96	465	533	445
93.25	0.248	0.96	596	592	564
94.25	0.193	0.99	576	576	574

Table 2: Evolution of the number of events in data and Monte Carlo as a function of cut in the charged lepton channel analysis. For the e^+e^- [16], $\tau^+\tau^-$ [15], $q\bar{q}$ [17] Monte Carlos, the number of generated events corresponds to an integrated luminosity equal to that of the data, while for the $\mu^+\mu^-$ [15] and four-fermion [19] Monte Carlos, it is 2.5 and 20 times larger respectively. The Monte Carlo expectation values have been normalized to the integrated luminosity of the data.

Cut	e^+e^- data	e^+e^- Monte Carlo	four-fermion Monte Carlo	$q\bar{q}$, $\tau^+\tau^-$ Monte Carlo	Efficiency, 3 GeV/c^2 H^0
$p_1 >$ 25 GeV/c, $p_2 >$ 15 GeV/c, electron ID	4851	4444.9	13.6	43.6	0.46
$0.10 < \alpha < 2.88$ rad.	59	66.9	1.9	0	0.19
radiation veto	3	6.1	1.9	0	0.19
conversion veto	1	0.9	1.9	0	0.19
$m_{vis} <$ 20 GeV/c^2	1	0.9	1.9	0	0.19
Cut	$\mu^+\mu^-$ data	$\mu^+\mu^-$ Monte Carlo	four-fermion Monte Carlo	$q\bar{q}$, $\tau^+\tau^-$ Monte Carlo	Efficiency, 3 GeV/c^2 H^0
$p_1 >$ 30 GeV/c, $p_2 >$ 20 GeV/c, muon ID	6021	6011.2	10.0	91.5	0.67
$0.10 < \alpha < 2.88$ rad.	75	74.6	1.4	1.2	0.34
radiation veto	11	4.2	1.3	1.2	0.34
conversion veto	7	0.8	1.3	1.2	0.34
$m_{vis} <$ 20 GeV/c^2	4	0.8	1.3	1.2	0.33

Table 3: Efficiency of charged lepton and neutrino channel analyses for Higgs bosons of masses between $2m_\mu$ and 15 GeV/c^2. For the neutrino channel, the 1 GeV/c^2 mass cut has not been applied.

M_H in GeV/c^2	$Z^{0*} \to e^+e^-$	$Z^{0*} \to \mu^+\mu^-$	$Z^{0*} \to \nu\bar{\nu}, H^0 \to \pi^0\pi^0$
0.21	0.13	0.19	0.40
3.00	0.19	0.33	0.50
7.00	0.22	0.37	0.52
12.00	0.21	0.38	0.53
15.00	0.20	0.40	0.53

Table 4: Classification of observed charged lepton channel events and comparison with the four-fermion Monte Carlo [19]. Cuts in the charged lepton channel analysis were loosened in order to be more sensitive to the process $Z^0 \to \ell^+\ell^- f\bar{f}$. Events are categorized as being e^+e^-X, $\mu^+\mu^-X$ if they satisfy the lepton identification criteria. The remaining events are classified as "$\tau^+\tau^-$ X" (see section 4).

Event Classification	Data	four-fermion Monte Carlo	Jetset 7.2 Monte Carlo ($Z^0 \to q\bar{q}$)
e^+e^-X	9	11.1	0
$\mu^+\mu^-X$	11	8.3	0
$\tau^+\tau^-X$	6	1.7	4.0

Table 5: Data and calculated backgrounds for events passing all cuts for the various MSM H^0 analysis regions and channels.

Channel	Data	Background
Charged Lepton:		
$m_{H^0} < 2m_\mu$	0	0
$m_{H^0} > 2m_\mu$	5	6.3 ± 1.6
Neutrino:		
$m_{H^0} < 3$ GeV/c^2	17	12.2 ± 1.1
$m_{H^0} > 3$ GeV/c^2	1	not considered

Figures

Figure 1: Weighted acoplanarity distribution α of the two highest momentum tracks after applying the lepton identification cuts for data, Monte Carlo simulation of $Z^0 \rightarrow \ell^+\ell^-(\gamma)$ events, and Monte Carlo simulation of $Z^0 \rightarrow e^+e^-(\mu^+\mu^-)H^0$ events for a Higgs boson of mass 3 GeV/c^2. The latter sample is equivalent to 25 times the integrated luminosity corresponding to the data.

Figure 2: Unassociated electromagnetic energy for data and Monte Carlo simulations of $Z^0 \rightarrow \ell^+\ell^-(\gamma)$ events removed by the $\ell^+\ell^-\gamma$, $\ell^+\ell^-\gamma\gamma$, and conversion veto in the charged lepton channel.

Figure 3: Energy deposited in the barrel electromagnetic calorimeter after all cuts in the neutrino channel analysis except the 4 GeV minimum barrel electromagnetic energy cut. (A preselection requirement of 2 GeV deposited energy was imposed on the data prior to applying the cuts described above.) Included on the plot is the expected distribution from $e^+e^- \rightarrow \nu\bar{\nu}\gamma$ events, and the distribution expected for a hypothetical 1 GeV/c^2 mass Higgs boson decaying entirely to $\pi^0\pi^0$. The distributions are normalized to the integrated luminosity.

Figure 4: 95% CL upper limit on a signal and the expected number of MSM Higgs bosons for (a) $m_H < 2m_\mu$ and (b) $m_H > 2m_\mu$. In (a), the 95% CL upper limit (dashed curve (D)) is a function of the H^0 mass (lifetime). Contributions from the neutrino and charged lepton channel are indicated by the solid curves (B) and (C) respectively. The sum is shown by the solid curve (A). In (b), the expected number of MSM Higgs bosons from the neutrino and charged lepton channel are indicated by the solid curves (A) and (B) respectively. The 95% CL upper limits for the two channels are indicated by the dashed curves (C) and (D) respectively. The expected levels for each channel assume a 100% branching fraction into the channel.

Figure 5: Upper limit on production of (a) MSM Higgs bosons, and (b) new scalars (S^0) that couple to the Z^0, given in terms of fractions of the decay width $\Gamma(Z^0 \rightarrow Z^{0*}H^0{}_{MSM})$. Also indicated in (b) (by the dashed line) is the upper limit on the production of h^0, the lightest Higgs scalar extensions of the Minimal Standard Model that contain more than one Higgs doublet. The decay $h^0 \rightarrow \tau^+\tau^-$ has been assumed.

Figure 1

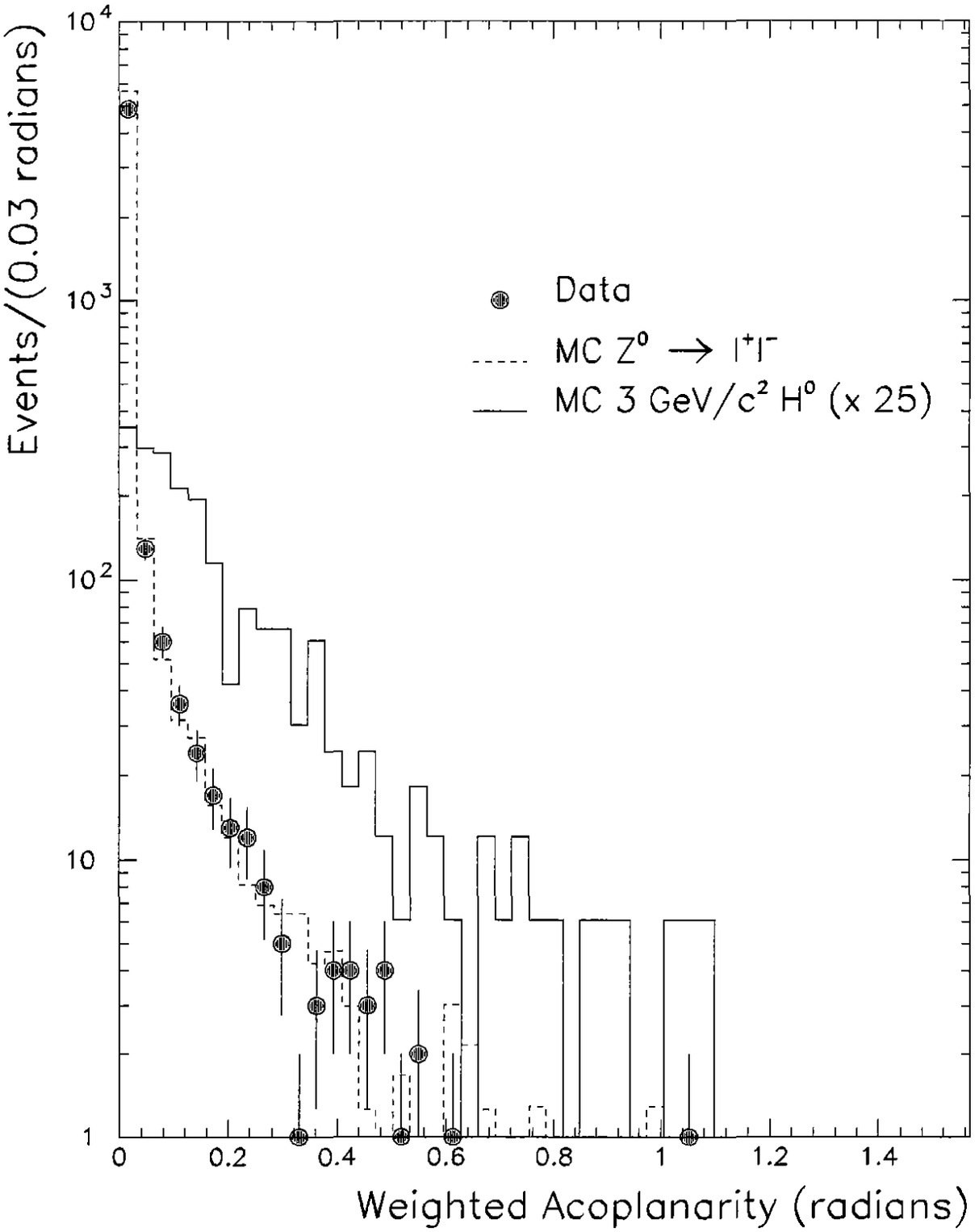
Events/(0.03 radians)
10^4
10^3
10^2
10
1
0
0.2
0.4
0.6
0.8
1
1.2
1.4
Weighted Acoplanarity (radians)
Data
MC $Z^0 \rightarrow l^+l^-$
MC 3 GeV/c^2 H^0 (x 25)

Figure 2

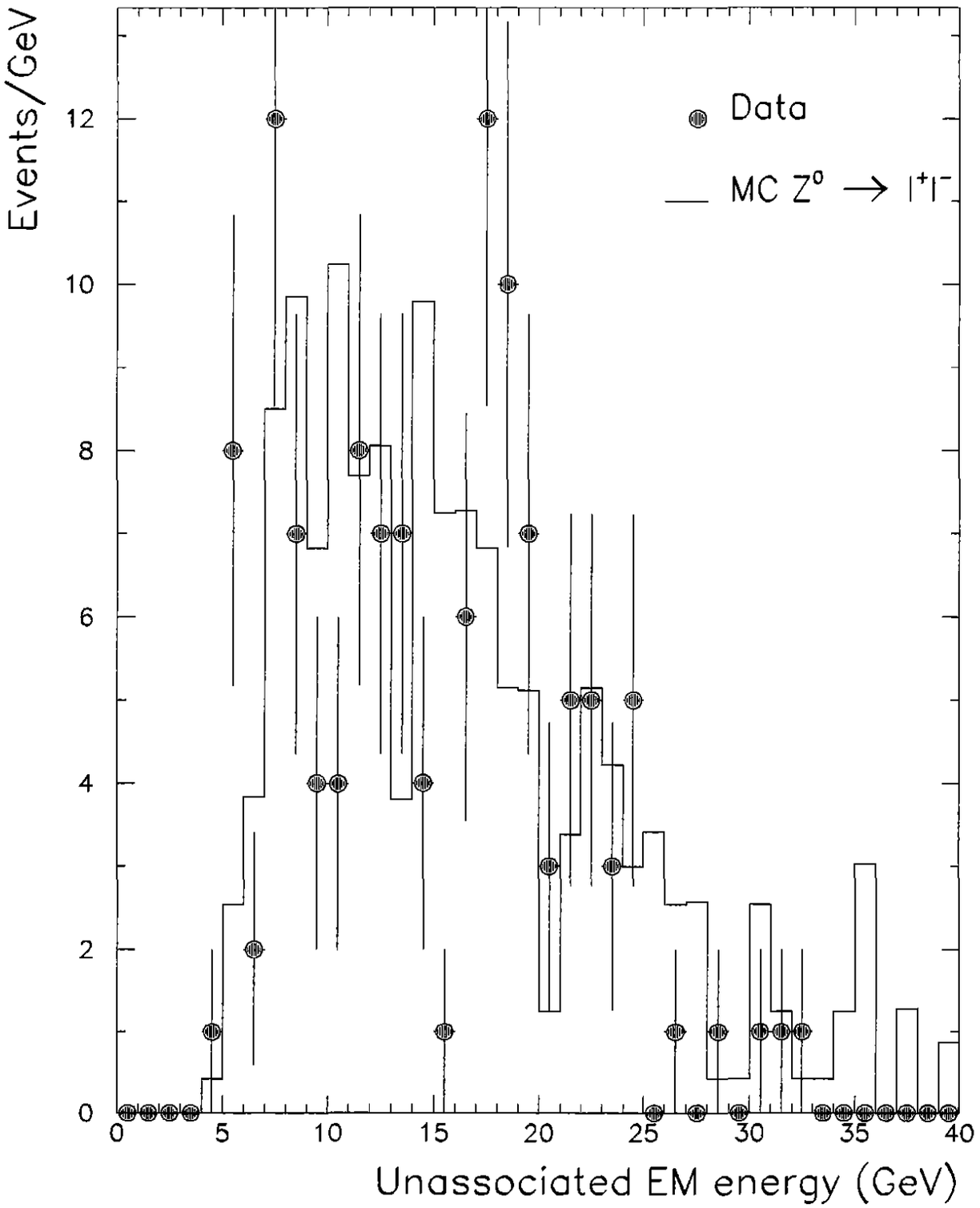
Events/GeV
Data
MC $Z^0 \rightarrow l^+l^-$
Unassociated EM energy (GeV)
0
2
4
6
8
10
12
0
5
10
15
20
25
30
35
40

Figure 3

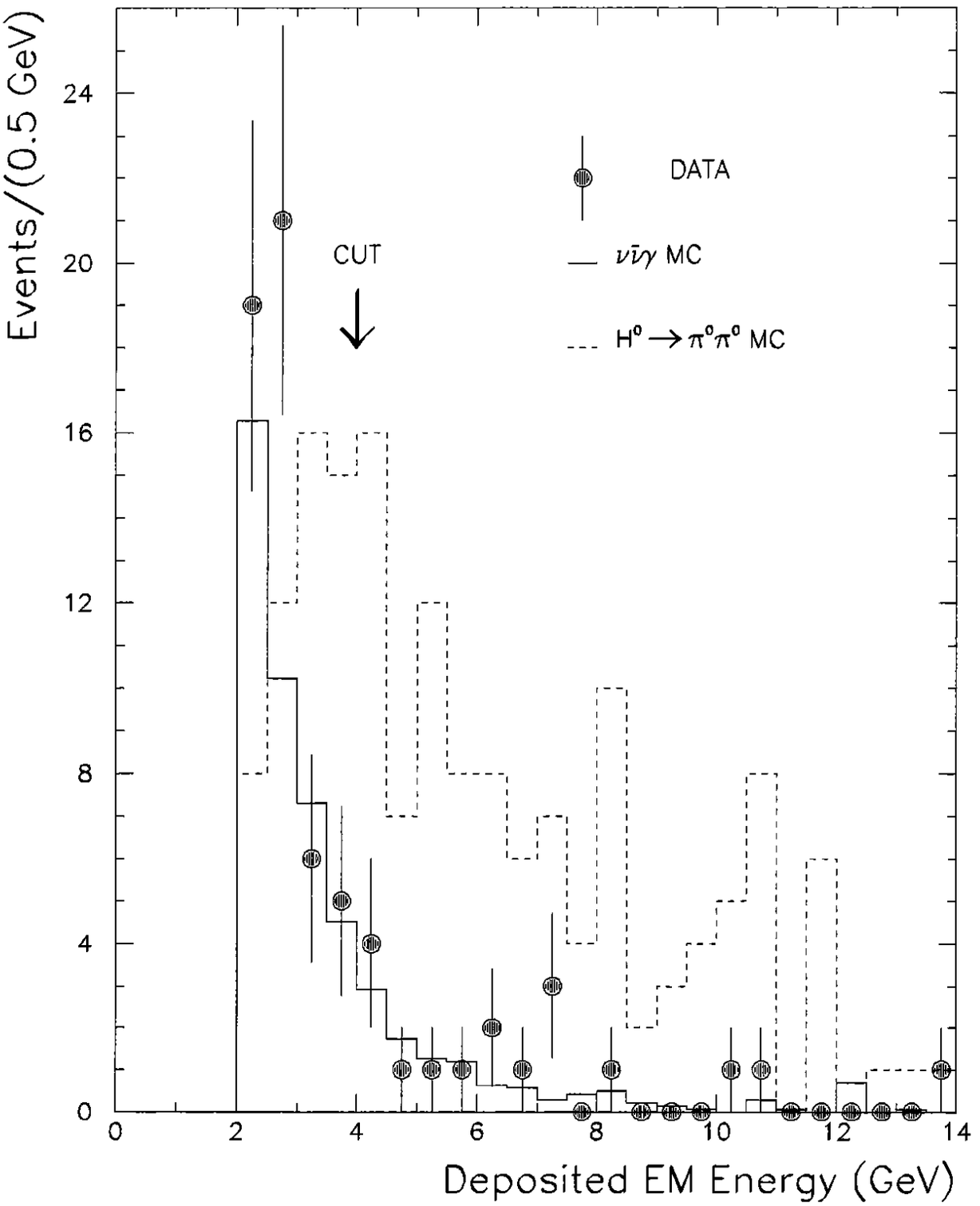
Events/(0.5 GeV)
24
20
16
12
8
4
0
0
2
4
6
8
10
12
14
Deposited EM Energy (GeV)
DATA
CUT
$\nu\bar{\nu}\gamma$ MC
$H^0 \rightarrow \pi^0\pi^0$ MC

Figure 4

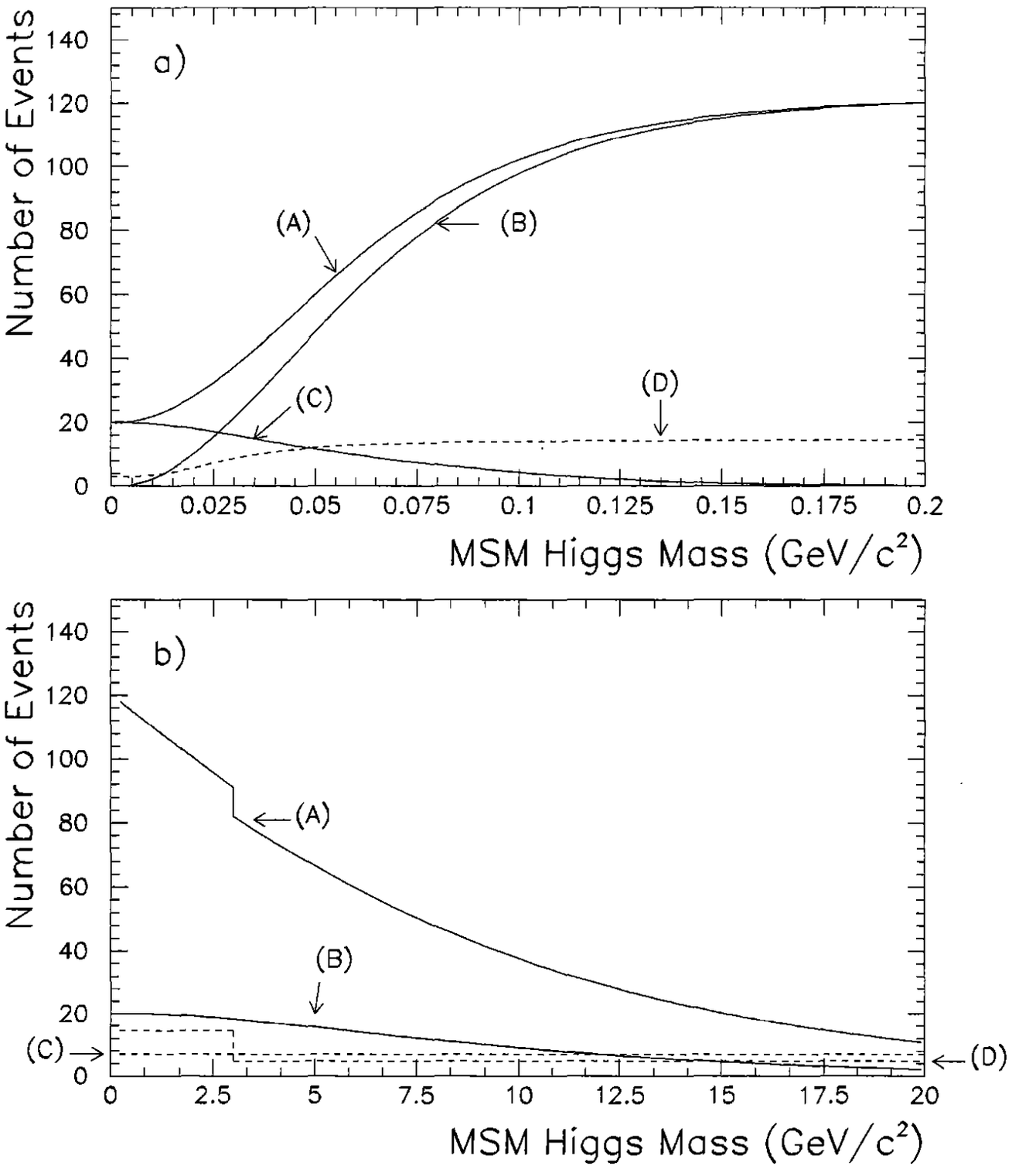
a)
Number of Events
140
120
100
80
60
40
20
0
(A)
(B)
(C)
(D)
0
0.025
0.05
0.075
0.1
0.125
0.15
0.175
0.2
MSM Higgs Mass (GeV/c²)
b)
Number of Events
140
120
100
80
60
40
20
0
(A)
(B)
(C)
(D)
0
2.5
5
7.5
10
12.5
15
17.5
20
MSM Higgs Mass (GeV/c²)

Figure 5

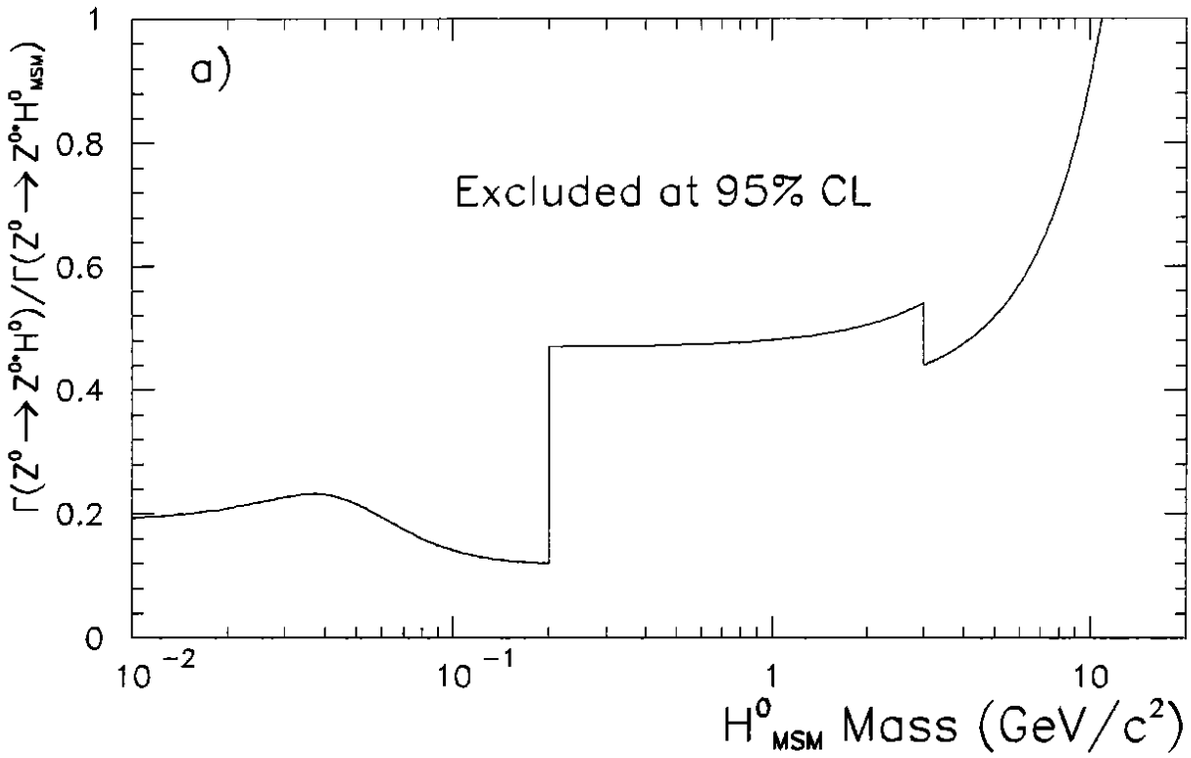
a)
Excluded at 95% CL
$\Gamma(Z^0 \to Z^{0*}H^0_{MSM})/\Gamma(Z^0 \to Z^{0*}H^0_{MSM})$
H^0_{MSM} Mass (GeV/c^2)
1
0.8
0.6
0.4
0.2
0
10^{-2}
10^{-1}
1
10

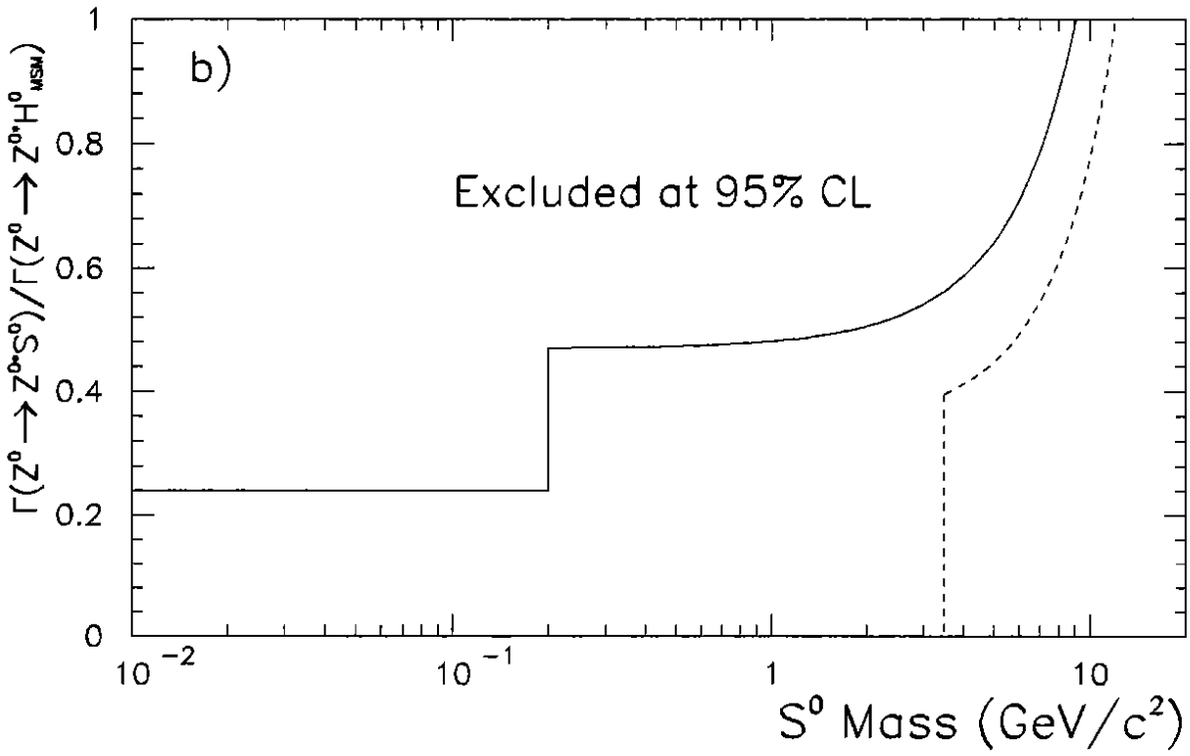
b)
Excluded at 95% CL
$\Gamma(Z^0 \to Z^{0*}S^0)/\Gamma(Z^0 \to Z^{0*}H^0_{MSM})$
S^0 Mass (GeV/c^2)
1
0.8
0.6
0.4
0.2
0
10^{-2}
10^{-1}
1
10